Onset of Corrosion Rate Retardation at Very Low Concentrations of H2S in a CO2 Environment

A. Cutright, B. Brown, S. Nesic, M. Singer, D. Young
Institute for Corrosion and Multiphase Technology
Department of Chemical & Biomolecular Engineering
Ohio University
Athens, OH 45701

ABSTRACT

Many experimental studies have indicated that the addition of H_2S on the order of 10^{-1} mbar to a CO_2 saturated environment can dramatically decrease the corrosion rate at various temperatures. This is likely due to the formation of a very thin layer of iron sulfide (FeS). In this research, the trend in corrosion rate of X65 steel at various H_2S concentrations below 100 ppm (0.1 mbar) in CO_2 at 1 bar total pressure and at various temperatures was studied. Corrosion rate was measured *in situ* using linear polarization resistance (LPR) and electrochemical impedance spectroscopy (EIS). It was observed that at 30°C, 0.5 ppm H_2S (0.0005 mbar pH_2S) had no effect on the corrosion rate compared to that seen in pure CO_2 conditions, whereas 5 ppm H_2S (0.005 mbar pH_2S) was able to significantly decrease the corrosion rate. At 80°C, a noticeable decrease was seen at 100 ppm, which was the highest concentration tested. The lack of a decrease in corrosion rate at 0.5 ppm at 30°C is likely due to the low concentration of H_2S molecules available leading to a slowing in the formation of the protective FeS layer. At 80°C, the corrosion rate is significantly higher leading to the necessity of increased H_2S concentrations to form the FeS layer fast enough to see a decrease in the corrosion rate.

Key Words: H_2S Corrosion; Souring

INTRODUCTION

Internal corrosion of mild steel pipelines is a major issue in the oil and gas industry, due to the presence of produced water in the oil and gas being extracted. Oil and gas reservoirs can be divided into two categories: sweet and sour. A sweet reservoir will have the dominant corrosive gas present be carbon dioxide (CO_2), whereas in a sour reservoir the hydrogen sulfide (H_2S) is in a significant enough quantity to have an effect on the corrosion. ISO 15156 states that for sulfide stress cracking, any system with $pH_2S > 3$ mbar was considered to be sour.[1] Several processes can lead to the presence of H_2S in the gas phase. For example, reservoir souring can refer to a situation where H_2S is being generated in a reservoir which was originally sweet or contained no H_2S and was dominated by CO_2. This can occur due to a variety of factors, the most common being biological souring where sulfate reducing bacteria (SRB) are introduced into the reservoir and begin to produce H_2S. It is also possible for the H_2S to already be present in the well, and be activated during the oil and gas extraction. The process of souring often presents as a slow increase in the H_2S content over time.[2] This means that, in a well which is originally sweet, at the onset of souring the environment in the pipeline will have a large amount of CO_2 with very small concentrations of H_2S present.

There have been studies looking at the trend in corrosion rate with low concentrations of H_2S in a CO_2 environment.[3,4,5] Previous research into the area of corrosion of mild steel has indicated that the corrosion rate is retarded when low concentrations of H_2S are present in a primarily CO_2 system.[3,4,5] This retardation in corrosion rate is attributed to the formation of thin layers of iron sulfide (FeS) on the metal surface which slow down the transfer of species to and from the surface. The kinetics of this layer formation process, expressed as scaling tendency (ST), was characterized previously as the ratio of the sulfide layer formation rate (SFR) and the underlying corrosion rate (CR), seen below in Equation 1.[6,7]

$$ST = \frac{SFR}{CR} \qquad (1)$$

This equation is valid when the precipitation and dissolution of the FeS layer play a significant role.[8] The SFR term refers to the likelihood of a protective layer being formed and is dependent on local conditions near the metal surface, including pH and the presence of both ferrous ions and sulfide species capable of forming FeS. The CR term is the underlying corrosion rate at the metal surface. It can be assumed that the retardation of the corrosion rate in the presence of small concentrations of H_2S can be linked with the value of ST. When the ST has a value greater than 1, this indicates that the formation rate (SFR) is higher than the corrosion rate (CR), so a layer can form which can retard the corrosion rate. If ST has a value lower than 1, the formation rate (SFR) is lower than the corrosion rate (CR), no significant layer formation will be seen, and the corrosion rate will not change.

When the H2S concentration is gradually increased from zero, in a sweet system, the corrosion rate is expected to eventually reach a minimum value and then begin to increase as the H_2S concentration is increased.[3,5] It has also been seen that temperature does not greatly affect this phenomenon, and the corrosion rate will be similarly decreased at similar concentrations of H_2S at different temperatures.[4] However, this previous work failed to go to low enough concentrations to sufficiently establish what trace concentrations of H_2S (<5 ppm) have an effect in the system. These studies[4] also did not consider other environmental parameters such as pH or fluid velocity and their effect on the system when looking at changes in temperature. The focus of this work is on very low concentrations of H_2S in a CO_2 system to observe which concentrations have no noticeable effect on the corrosion rate. Additionally, a change in the temperature of the experimental system was used to observe its influence on these low concentrations of H_2S that can be present in the system.

EXPERIMENTAL PROCEDURE

A three-electrode glass cell setup, which can be seen below in Figure 1, was used to conduct corrosion experiments at pH 4.0, 1 bar, 30°C and 80°C. The electrolyte used was a 1 wt% NaCl solution. The steel sample used was an X65 steel rotating cylinder electrode (RCE) rotated at 1000 rpm; this was the working electrode. The counter electrode was a platinum covered titanium mesh, with a saturated KCl, Ag/AgCl electrode connected via a Luggin capillary acting as the reference electrode. The reference electrode was maintained at room temperature throughout these experiments using the Luggin capillary. The pH in the system was maintained at 4.0±0.05 for the duration of each experiment. The system was purged with a mixture of CO_2 and H_2S using a system of rotameters to control the flowrates of the gases, and a Gastec[†] pump and detector tubes were used to measure the concentration of H_2S in the gas entering the glass cell. Concentrations tested in this work at 30°C and 80°C are shown below in Table 2. The glass cell was purged for at least one hour prior to introduction of the RCE specimen, which was polished using 600 grit sandpaper until no polishing marks were visible on the sample. Once the sample was inserted into the glass cell, a 1-hour open circuit potential (OCP) measurement was performed to allow the system to stabilize at the corrosion potential. Following this, linear polarization resistance (LPR) measurements were performed every 30 minutes for 4 hours by polarizing the sample from -5 mV to +5 mV from the corrosion potential. Finally, electrochemical impedance spectroscopy (EIS) was performed to determine the solution resistance by scanning a frequency range from 10000 to 0.01 Hz. The corrosion rate was calculated using a *B* value of 26 mV/decade.

[†]Trade name.

1. Reference Electrode (RE – Saturated Ag / AgCl)
2. Rotating Cylinder Electrode (WE)
3. Counter Electrode (CE)
4. Luggin Capillary
5. pH Meter
6. Thermocouple
7. Gas in
8. Gas out
9. Magnetic Stirrer
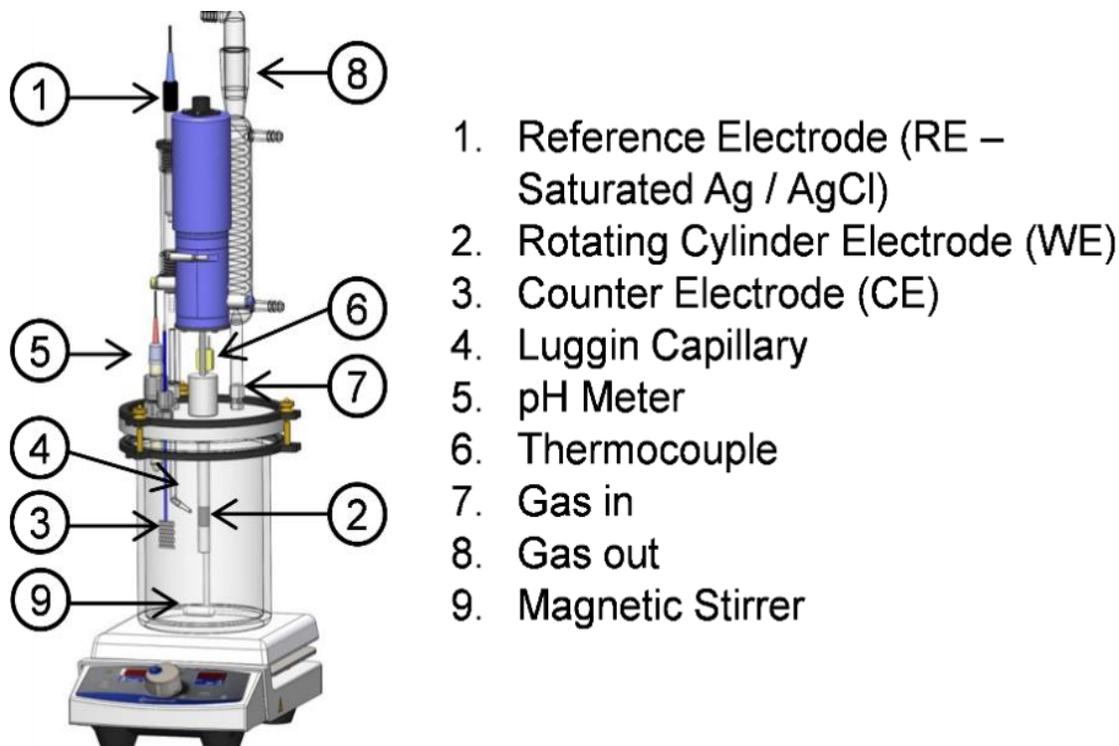
Figure 1. Three-electrode system in a 2-liter glass cell was used for experiments. [1]

Table 1
API 5L X65 Steel Composition

C	Mn	Nb	P	S	Ti	V	Fe
0.05%	1.51%	0.03%	0.004%	<0.001%	0.01%	0.04%	balance

Table 2
Summary of Experimental Conditions

Description	Parameters
Solution	1 wt. % NaCl
Temperature / °C	30, 80
RCE rotating speed	1000 rpm
pH	4.0 ± 0.05
H_2S concentrations / ppm	0, 0.5, 5, 50, 100
H_2S concentrations / mbar	0, 0.0005, 0.005, 0.05, 0.1
Electrochemical techniques	LPR, EIS, OCP

[1] Image taken from Cody Shafer, ICMT, Athens OH

RESULTS AND DISCUSSION

The first set of conditions tested was at 30°C and included concentrations of H_2S of 0, 0.5, 5, and 50 ppm. Shown below in Figure 2 is the average corrosion rate calculated using the LPR data in mm/year *vs* H_2S concentration.
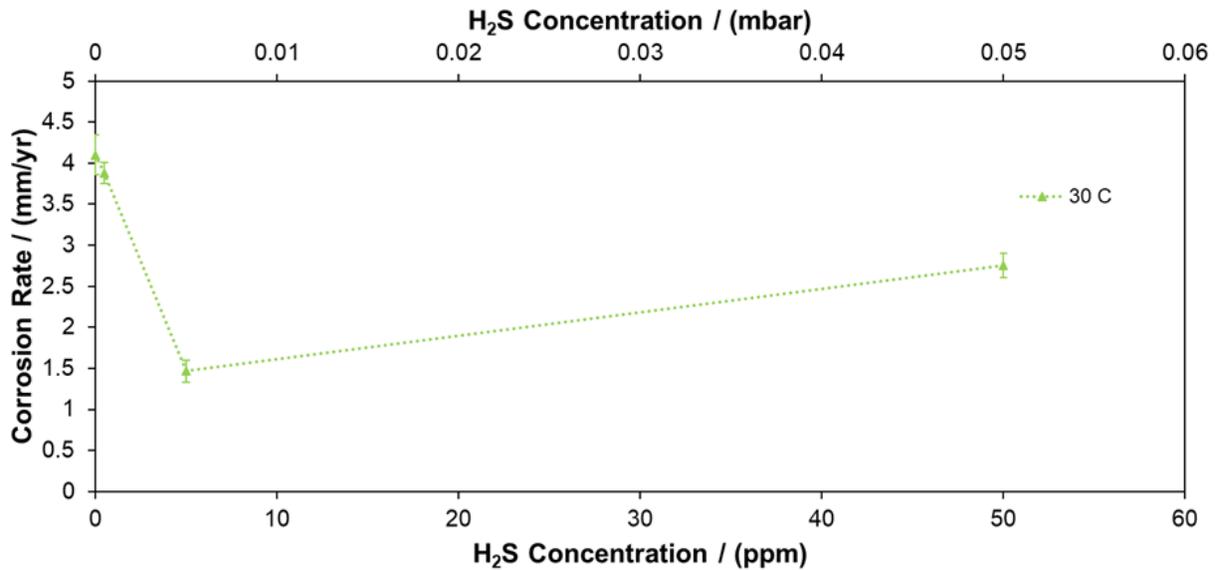
Figure 2: Average corrosion rate as a function of H_2S gas phase concentration in solution at 30°C, 1 wt% NaCl, 1000 rpm RCE, 0.97 bar pCO_2, B = 26mV.

From the data shown in Figure 2, it can be seen that there was no significant difference in the corrosion rates at 0.5 ppm H_2S and pure CO_2, which would correspond to ST < 1 as defined by Equation 1.[6,7] However, at 5 ppm there was a noticeable decrease in the average corrosion rate which corresponds to ST > 1. This indicates that, at the condition tested, concentrations at and below 0.5 ppm H_2S had no impact on the corrosion rate as compared to the pure CO_2 corrosion rate under the same environmental conditions. However, at 5 ppm H_2S the corrosion rate decreased dramatically as would be expected based on previous work.[3]

Similar experiments were then performed with the system temperature at 80°C, the results of these experiments can be seen below in Figure 3.
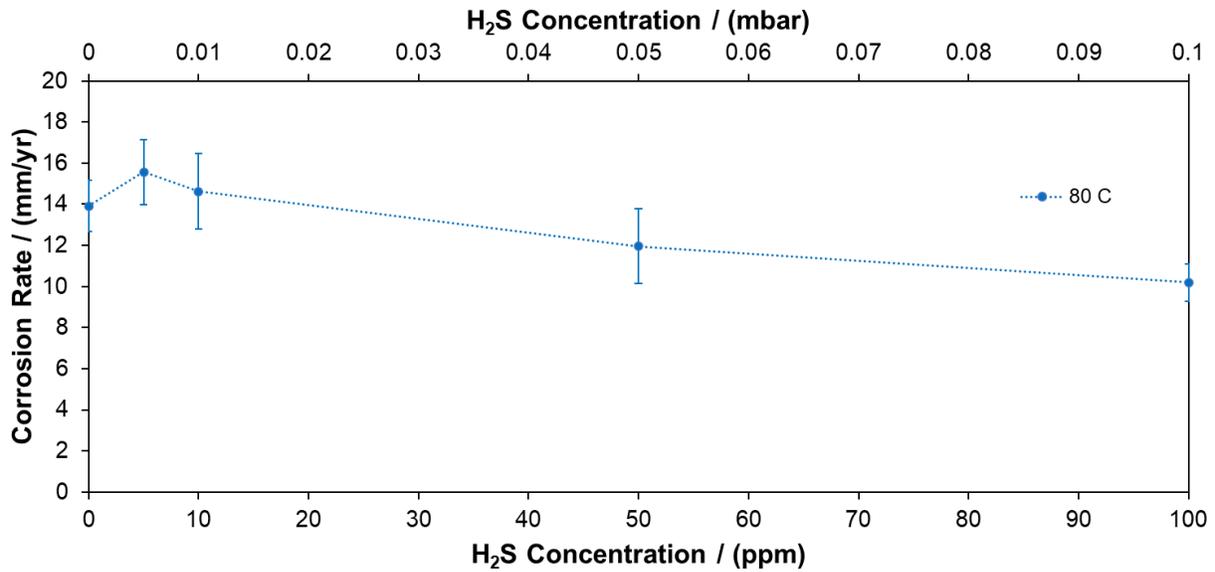
Figure 3: Average corrosion rate as a function of H_2S gas phase concentration in solution at 80°C, 1 wt% NaCl, 1000 rpm RCE, 0.53 bar pCO_2, B = 26mV.

The data show that there was no significant decrease in the corrosion rate compared to pure CO_2 until 100 ppm H_2S was present in the system. This was a gas concentration 20 times higher than was needed at 30°C to see a decrease in the corrosion rate. This difference was likely the result of the significant increase in the baseline corrosion rate from 30°C to 80°C which would then be greater than the SFR, leading to ST < 1. With the much higher baseline corrosion rate, it would be expected that a protective layer would have to form significantly faster to see a decrease in the corrosion rate. The sets of experiments at 30°C and 80°C are displayed together in Figure 4.
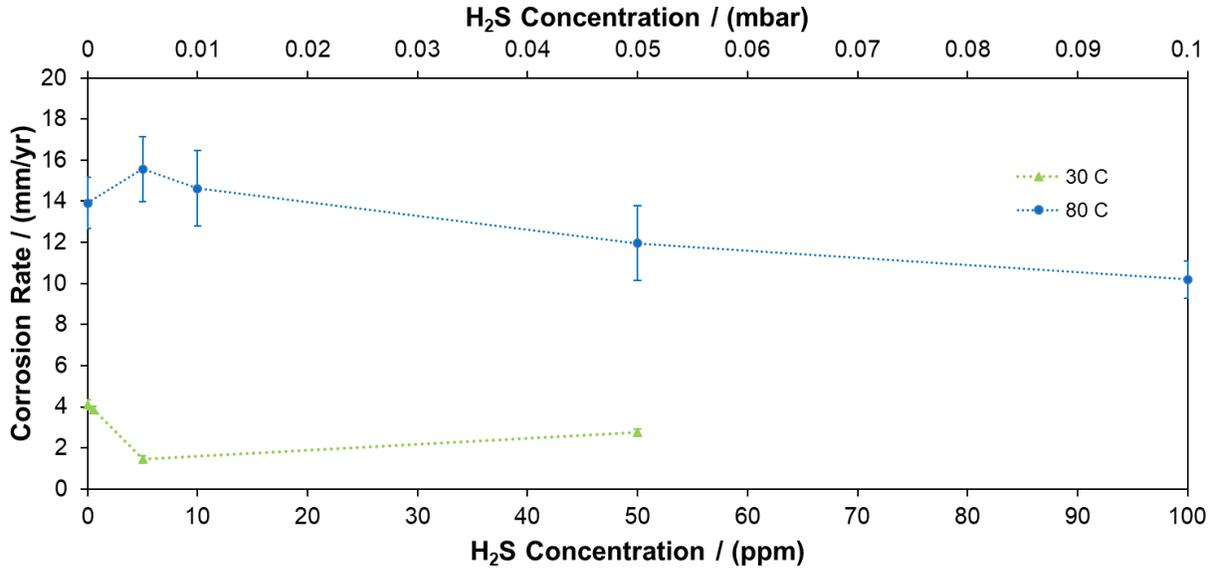
Figure 4: Average corrosion rate as a function of H₂S gas phase concentration at 30°C and 80°C, 1 wt% NaCl, 1000 rpm RCE, 0.53 bar pCO₂, B = 26mV.

One important factor to note is that the concentrations being compared are gas phase concentrations of H₂S. The corrosion rates should also be compared using aqueous phase concentrations of H₂S, given that the solubility of gaseous H₂S in water is temperature dependent. This can be accounted for by using Henry's Law with the appropriate constants for H₂S and water. Henry's Law used for this calculation and the associated constants can be seen below in Equation 2[9] and Table 3 respectively. The data comparison can be seen below in Figure 5.

$$k_H = k^0{}_H \times \exp\left(\frac{-d\,ln(k_H)}{d\left(\frac{1}{T}\right)} * \left(\frac{1}{T} - \frac{1}{T^0}\right)\right) \tag{2}$$

Table 3
Constants used for Henry's Law calculation[9]

$k^0{}_H$/ (M/atm)	$\frac{-d\,ln(k_H)}{d\left(\frac{1}{T}\right)}$/ (K)	T^0/ (K)
0.087	2100	298.15

Table 4
Comparison of gas and aqueous phase concentrations at 30°C and 80°C

Gas Phase H_2S Concentration / (ppm)	Aqueous H_2S Concentration / (M)	
	30°C	80°C
0.5	3.87×10^{-8}	1.45×10^{-8}
5	3.87×10^{-7}	1.45×10^{-7}
10	7.75×10^{-7}	2.90×10^{-7}
50	3.87×10^{-6}	1.45×10^{-6}
100	7.75×10^{-6}	2.90×10^{-6}
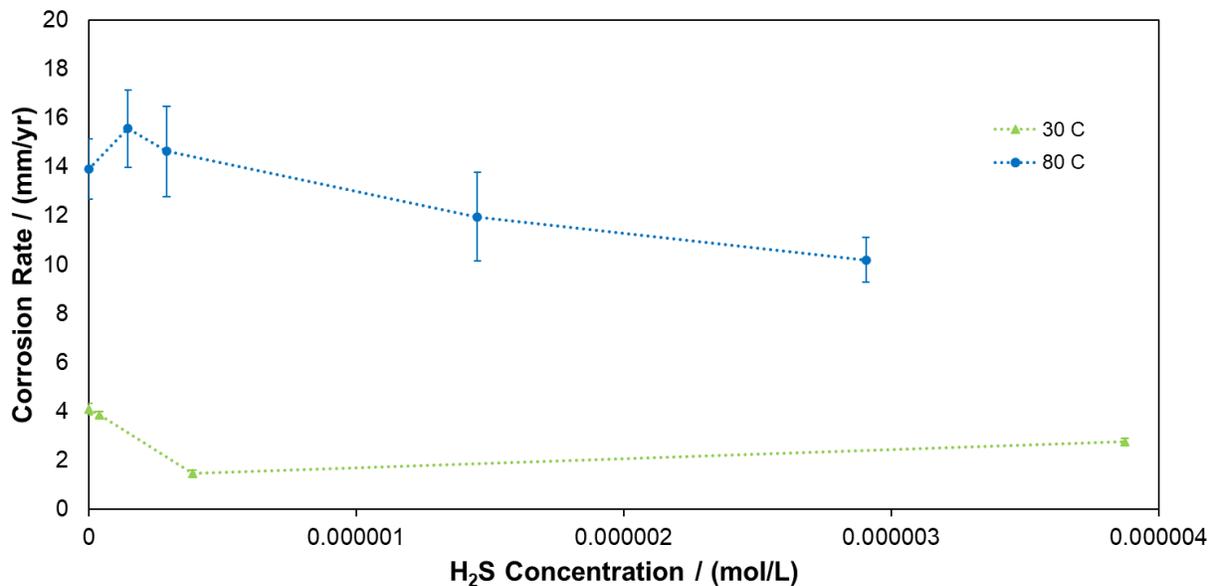
Figure 5: Average corrosion rate as a function of aqueous H_2S concentration at 30°C and 80°C, 1 wt% NaCl, 1000 rpm RCE, 0.53 bar pCO_2, B = 26mV.

Figure 5 confirms that, at higher temperature, higher concentration of H_2S was required to decrease the corrosion rate as compared to the corrosion rate in a pure CO_2 environment. Additionally, the contribution of the temperature change to the solubility of H_2S in the aqueous phase does not fully account for the differences in required H_2S concentration to see a decrease in the corrosion rate compared to the pure CO_2 environment. Although the reason behind this observation must be linked to the protectiveness of the FeS layer, a comprehensive mechanistic explanation of this phenomenon is still largely elusive.

Based on these results, low concentrations of H_2S are unable to decrease the corrosion rate from the value seen at pure CO_2 conditions as was expected. Additionally, while reactions rates and precipitation rates should dramatically increase with a temperature increase from 30°C to 80°C, the fact that no retardation of the corrosion rate was seen

indicates that the increase in the kinetics of the formation rate are being offset by the increase in the corrosion rate leading to ST < 1. This was indicated by the fact that at similar gas and aqueous phase concentrations of H_2S between the two temperatures, the decrease in corrosion was significantly different. Much higher concentrations of H_2S must be present at the higher temperature to see a decrease in the corrosion rate.

CONCLUSIONS

At low temperatures, 0.5 ppm H_2S in a CO_2 system was unable to cause a significant decrease in the corrosion rate; this was likely due to the FeS precipitation rate being too low (due to the low H_2S concentration) to compete with the undermining substrate corrosion rate; this would correspond to ST < 1. With 5 ppm H_2S in the system, the corrosion rate was retarded as expected based on previous work. In this case, the higher H_2S content led to a higher FeS precipitation rate, generating a more protective layer, corresponding to ST > 1. When the temperature in the system was increased, the corrosion rate increased dramatically, which was accompanied by an increase in the FeS precipitation rate. However, based on the results seen in Figure 5 comparing the two different sets of experiments, the undermining corrosion rate at a higher temperature was hypothesized to be too high to allow for the retention of a protective FeS.

ACKNOWLEDGMENTS

REFERENCES

1. NACE MR0175/ ISO 15156-1. "Petroleum and natural gas industries - Materials for use in H_2S-containing Environments in oil and gas production" (Houston, TX: NACE)
2. J. Mi, B. Zhang, Z. Shen, W. Huang, A. Casalins, C. Liu "The experimental study on H_2S generation during thermal recovery process for heavy oil from the Eastern Venezuela Basin," *Journal of Natural Gas Geoscience* 2, 3 (June 2017): pp. 201-208.
3. Y. Zheng, Electrochemical Mechanism and Model of H_2S Corrosion of Carbon Steel. Ph.D. Thesis, Ohio University, May 2015.
4. Lee, J. K.-L. A Mechanistic Modeling of CO_2 Corrosion of Mild Steel in the Presence of H_2S. Ph.D. Thesis, Ohio University, November 2004.

5. K. Videm, J. Kvarkeval "Corrosion of Carbon Steel in Carbon Dioxide-Saturated Solutions Containing Small Amounts of Hydrogen Sulfide," *Corrosion* 51, 4 (April 1995): pp. 260-269.
6. W. Sun, Kinetics of Iron Carbonate and Iron Sulfide Scale Formation in CO_2/H_2S Corrosion. Ph.D. Thesis, Ohio University, November 2006.
7. E. W. J. van Hunnik, B.F. M. Pots, and E. L. J. A. Hendriksen, The formation of protective FeCO3 corrosion product layers in CO2 corrosion, Corrosion/96, paper no. 6, NACE International, Houston, Texas, 1996.
8. S. Nesic, Y. Zheng, B. Brown, J. Ning, "Advancement in Predictive Modeling of Mild Steel Corrosion in CO_2 and H_2S Containing Environments," NACE, 6146 (Houston, Texas: NACE International, 2015) pp. 1-20.
9. R. Sander: Compilation of Henry's law constants (version 4.0) for water as solvent, Atmos. Chem. Phys., 15, 4399–4981, https://doi.org/10.5194/acp-15-4399-2015, 2015.